Selective disruption of the mammalian secretory apparatus enhances or eliminates calcium current modulation in nerve endings

Eugene M. Silinsky*

Department of Molecular Pharmacology and Biological Chemistry, Northwestern University Medical School, 303 East Chicago Avenue, Chicago, IL 60611

Edited by Thomas C. Südhof, University of Texas Southwestern Medical Center, Dallas, TX, and approved February 29, 2008 (received for review September 17, 2007)

Modulation of secretion via G protein-coupled receptors (GPCRs) serves an important regulatory function in neuronal and nonneuronal secretory cells. Most secretory cells possess voltage-gated calcium channels, share homologues of the core complex of three proteins (the SNAREs) that constitute the secretory apparatus, and are modulated by GPCR activation. Activators of GPCRs generally inhibit the release of neurotransmitter substances to a maximum of only 50–60% of the control level, suggesting that complex protein–protein interactions may govern the efficacy of this form of modulation. In this article, molecular genetic approaches are used in combination with botulinum toxins (selective molecular scalpels that cleave the SNAREs at highly restricted loci) to address this issue. The results suggest that the cleavage of either of the plasma membrane SNAREs (syntaxin or SNAP-25) prevents modulation of calcium currents by A_1 adenosine receptors at mammalian motor nerve endings. In contrast, cleavage of the synaptic vesicle SNARE (synaptobrevin) in conjunction with deletion of the vesicle-docking protein Rab3A greatly enhances the efficacy of calcium current modulation.

adenosine | neuromuscular junction | neurotransmitter release | synaptic vesicles

The fine regulation of the levels of neurotransmitter output by endogenous substrates occurs at most synapses and is mediated via G protein-coupled receptors (GPCRs) on the nerve terminal (1–3). Such modulation may be mediated through effects on the entry of Ca^{2+} through Ca^{2+} channels into the nerve terminal (4, 5) and through actions on the secretory apparatus independently of effects on Ca^{2+} channels (1–3, 6–10). As a general rule, the maximal inhibitory effect of the endogenous substrate is often limited to ≈50% of the control level (1–3, 11, 12), but some GPCR agonists may have greater efficacies as inhibitors of neurotransmitter release (12).

At the skeletal neuromuscular junction, the endogenous GPCR agonist adenosine acts as an inhibitor of neurotransmitter release and is responsible for neuromuscular depression at amphibian (7, 13–15) and mammalian (4, 16, 17) synapses. Indeed, at amphibian synapses, adenosine derived from vesicular ATP (18) appears to be the exclusive mediator of prejunctional neuromuscular depression in response to low-frequency (0.1–10 Hz) nerve stimulation (7, 15). A_1 adenosine receptor activation inhibits neurotransmitter release in amphibians by an effect on strategic components of the secretory apparatus and not by effects on membrane ionic channels (3, 6–8, 15).

In contrast to the amphibian results, A_1 adenosine receptor activation causes simultaneous decreases in both P/Q type Ca^{2+} currents and the evoked release of the neurotransmitter acetylcholine (Ach) at mouse motor nerve endings (5). Despite this effect on Ca^{2+} currents, studies with botulinum toxins suggest that the three members of the core complex of the secretory apparatus (the SNAREs) play important roles in mediating the effects of adenosine at mouse motor nerve endings (19–24). Botulinum toxins (Botxs) are a family of zinc-dependent metalloendopeptidases that abolish Ach release by selectively cleaving individual SNAREs at highly restricted loci. As Fig. 1 shows, the three SNAREs form a tight helical bundle in which a complex of the two nerve terminal SNAREs (t-SNARES), syntaxin (red) and SNAP-25 (synaptosomal associated protein of 25 kDa, green), is joined by the vesicle SNARE (v-SNARE) synaptobrevin (darker blue) to form a primed vesicle. Botulinum toxin type C (Botx/C) cleaves syntaxin (see Fig. 1), an integral presynaptic membrane protein intimately linked to Ca^{2+} channels (19, 21) (Fig. 1, Ca^{2+} channels), and eliminates the inhibitory effects of adenosine on Ca^{2+} currents at mouse motor nerve endings (19). In addition, genetic deletion of the small GTP-binding protein Rab3A (Fig. 1, light blue), a synaptic vesicle protein implicated in both synaptic vesicle recycling and vesicle docking (17, 20), alters presynaptic modulation. Specifically, adenosine has an increased potency as an inhibitor of both Ca^{2+} currents and evoked Ach release in the Rab3A$^{-/-}$ mutant mouse (5, 17). This result raises the possibility that Rab3A, either on its own or via an interaction with its binding partners RIM (Rab interacting molecule; Fig. 1, yellow) or rabphilin (not shown), provides a negative regulatory control on the potency of GPCR agonists by altering the conformation of the SNARE–Ca^{2+}channel complex.

Because docking via Rab3A reduces the potency of adenosine, it is of interest to investigate whether cleavage of the SNAREs in the Rab3A$^{-/-}$ deletion mutant alters the efficacy of GPCR agonists. To perform these studies, botulinum toxins were used to cleave individual SNARE proteins (21–24). The modulatory effects of adenosine on Ca^{2+} currents after disruption of the SNAREs were then examined in Rab3A$^{-/-}$ mutant and compared with the effects of similar treatments in the wild-type mouse.

Results

General Observations on the Effects of Adenosine in the Rab3A$^{-/-}$ Mutant as Compared with the Wild-Type Mouse. The inhibition of both Ca^{2+} currents and evoked Ach release by adenosine may be measured simultaneously at the mouse neuromuscular junction (5). Fig. 2*A* shows an example of the typical presynaptic ionic currents (upper traces) recorded simultaneously with evoked Ach release [end-plate potentials (EPPs), lower traces] in the Rab3A$^{-/-}$ mutant in the absence of toxin treatment. As shown in Fig. 2*A* (upper traces), the downward waveform represents the Na^+ current produced by Na^+ influx in the nodes of Ranvier and

Author contributions: E.M.S. designed research, performed research, analyzed data, and wrote the paper.

The author declares no conflict of interest.

This article is a PNAS Direct Submission.

*To whom correspondence should be addressed. E-mail: e-silinsky@northwestern.edu.

This article contains supporting information online at www.pnas.org/cgi/content/full/0708814105/DCSupplemental.

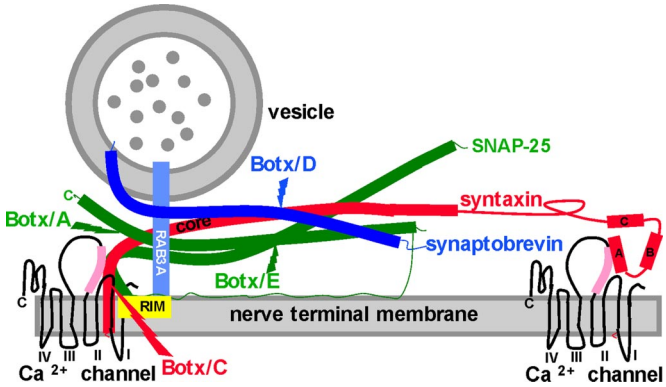

Fig. 1. The secretory apparatus and the cleavage sites for Botxs. The SNAREs syntaxin (red), SNAP-25 (green), and synaptobrevin (darker blue) are shown in their primed state based on the crystal structure of the complex, as are the cleavage sites for Botx/A, C, D, and E (38). Some liberty has been taken with respect to the distance between vesicle and nerve terminal membrane and with the relative sizes of the HABC domains of syntaxin for illustrative purposes in this figure and in Fig. 5. For syntaxin, the helical core domain (core, also termed the H3 domain) contributes one helical domain to the parallel four-helix bundle of the primed SNAREs, with SNAP-25 (two helices) and synaptobrevin (one helix) constituting the rest of the bundle. Recent publications provide strong evidence that the Hcore domain is the likely target for GPCR activation (10, 32). The other three N-terminal helices of syntaxin (HA, B, and C) do not contribute to the SNARE complex. The reported interactions of the HA domain (32) and the Hcore (H3) domains (35) with the synprint region (pink) of P/Q- and N-type Ca^{2+} channels are both depicted. The synprint region and the P/Q Ca^{2+} channel structure were drawn in accordance with refs. 28–32. Also shown is GTP-bound Rab3A (lighter blue) interacting with RIM (yellow). Synaptotagmins (20), which are the Ca^{2+} sensors that mediate the action of Ca^{2+} once this divalent cation has entered the nerve ending via voltage gated Ca^{2+} channels, are not shown.

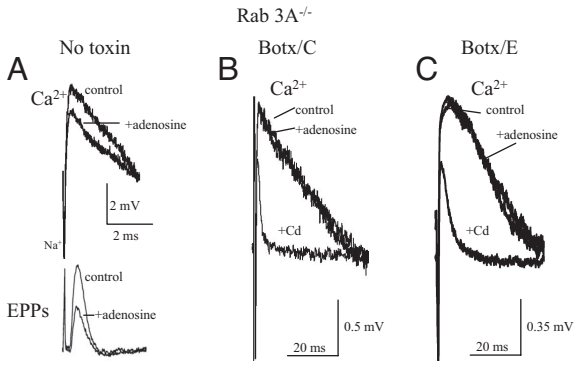

Fig. 2. The effects of adenosine in the Rab3A$^{-/-}$ mutant in the absence of botulinum toxin treatment (*A*) and after cleavage of syntaxin with Botx/C (*B*) and SNAP-25 with Botx/E (*C*). (*A*) Typical effect of supramaximal concentrations of adenosine (10 mM) in the absence of botulinum toxins on perineural calcium currents (Ca^{2+}, upper traces) and Ach release (EPPs, lower traces) recorded under the same conditions. See *Materials and Methods* for details of the polarities of the waveforms and description of the perineural currents, which are reflected as voltage changes in the extracellular compartment and are thus calibrated in millivolts. Dose–response relationships for adenosine as an inhibitor of Ach release and calcium currents in both normal and Rab3A$^{-/-}$ deletion mutants have been previously published by this laboratory (5, 17). Because the efficacy, not the potency, of adenosine was to be examined, and for comparison with previously published results (see figure in ref. 5), supramaximal concentrations of adenosine (10 mM) were used in all experiments in this study. (*B*) Cleavage of syntaxin with Botx/C eliminates the inhibitory effect of adenosine (the averaged peak perineural waveform was 1.1 mV in both control and adenosine traces in *A*, $n = 5$ responses averaged) but not that of Cd^{2+} on Ca^{2+} currents. (*C*) Cleavage of SNAP-25 with Botx/E eliminates the inhibitory effect of adenosine (the averaged peak perineural waveform was 1.2 mV in both control and adenosine traces in *B*, $n = 9$–12 responses averaged), but not that of Cd^{2+}, on Ca^{2+} currents.

the terminations of the myelin sheaths (25–29) (Fig. 2*A*, Na^+). The upward deflections (Fig. 2*A*, Ca^{2+}) reflect the movement of Ca^{2+} through P/Q-type calcium channels as these waveforms are inhibited by ω-agatoxin IVA or Cd^{2+} (5, 19, 25–29). Fig. 2*A* shows the typical maximal inhibitory effect of adenosine in the absence of SNARE cleavage. In this experiment, adenosine inhibits the Ca^{2+} current to 77.5% of control and concomitantly inhibits the EPP to 50% of the control level (Fig. 2*A*, lower traces, $P < 0.035$). In all experiments using normal Ca^{2+} solutions, supramaximal concentrations of adenosine inhibited Ca^{2+} currents to 75.9% ± 3.1% of the control level ($n = 6$ experiments) in the Rab3A$^{-/-}$ mutant. This inhibitory effect is indistinguishable from the maximal effects of adenosine on calcium currents in wild-type mice (75.4% ± 3.9%, mean ± 1 SEM, $n = 5$ experiments). Fig. 2*A* also shows that this maximal inhibitory effect of adenosine on Ca^{2+} currents is associated with a decrease in evoked Ach release to ≈50% of control (51.8% ± 2.3%, $n = 5$ experiments) (5, 17). Fig. 3 (Control) shows mean data for the maximal level of inhibition of calcium currents by adenosine for the wild-type mouse (wt, open bars) and the Rab3A$^{-/-}$ mutant (black bars) in the absence of toxin treatment.

Cleavage of Syntaxin Eliminates the Effects of Adenosine. Next, the roles of various components of the SNARE complex in mediating the effects of adenosine on Ca^{2+} currents were investigated by using specific botulinum toxin serotypes. Treatment of mouse phrenic nerve hemidiaphragm preparations with Botx/C selectively cleaves syntaxin between amino acids K^{253} and A^{254} near the transmembrane region of this SNARE (Fig. 1), eliminates syntaxin immunoreactivity, and blocks evoked neurotransmitter release (19, 24). As Fig. 2*B* shows, after Botx/C treatment in the Rab3A$^{-/-}$ mutant, the presynaptic Ca^{2+} current is not affected by adenosine. This concentration of adenosine is ≈20-fold higher than the concentration that produces a maximal inhibitory effect in the Rab3A$^{-/-}$ mutant (5, 17). In contrast, Cd^{2+}, which acts by blocking the calcium entry pore, produced its typical inhibitory effect on Ca^{2+} currents after syntaxin cleavage by Botx/C (Fig. 2*B*, Cd^{2+}). In all five experiments made after complete blockade of Ach release by Botx/C treatment, no

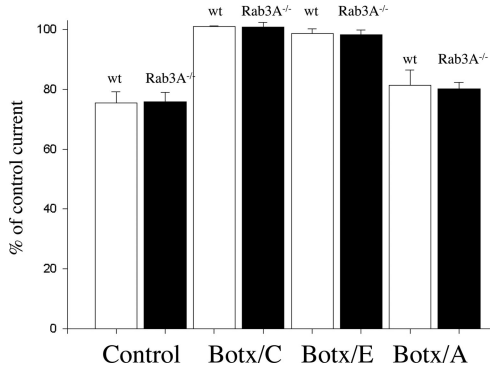

Fig. 3. Effects of adenosine after cleavage of t-SNAREs in the Rab3A$^{-/-}$ mutant mouse (filled bars) as compared with the wild-type mouse (open bars). In control preparations (no botulinum toxins), neuromuscular transmission was blocked by 25–50 μM Tubocurarine, whereas for the Botx fractions, transmission was blocked prejunctionally by cleavage of the SNAREs with the particular Botx serotype. Each bar represents the average percent inhibition for five or six different experiments. With the exception of the Botx/E experiments, data from wild-type mice were taken from ref. 19. Note that supramaximal concentrations of adenosine failed to inhibit P/Q Ca^{2+} currents after cleavage of syntaxin with Botx/C or SNAP-25 with Botx/E in either the wild-type or Rab3A$^{-/-}$ mutant mouse. *P* values ranged from 0.13 to 0.94 in the individual experiments.

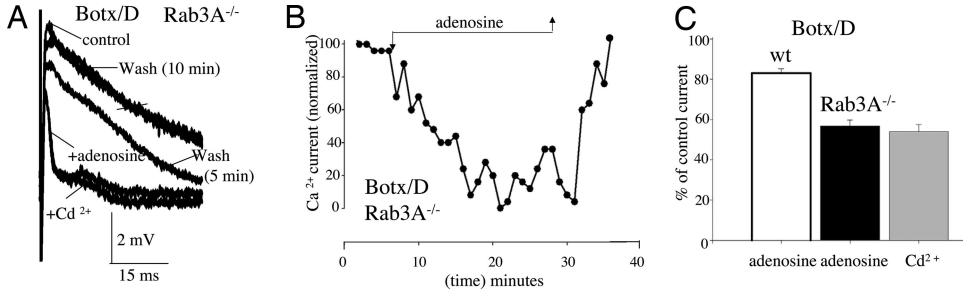

Fig. 4. Increased efficacy of adenosine in the Rab3A$^{-/-}$ mutant after cleavage of the vesicle protein synaptobrevin with Botx/D. (*A*) Raw traces (each trace is the average of three to six stimuli, 0.017 Hz). Note the complete and reversible inhibition of Ca^{2+} currents by adenosine and its similarity to the effects of Cd^{2+}. (*B*) Inhibition by adenosine of the normalized peak Ca^{2+} current. Each point is the response to a single stimulus. To normalize the peak Ca^{2+} current, the residual outward Cd^{2+}-insensitive component (a component that is independent of Ca^{2+} entry via presynaptic Ca^{2+} channels; see refs. 5 and 29) was subtracted from peak currents. This residual outward current after Cd^{2+} is likely to be due to the Na^{+} current associated with the action potential, a current that passively repolarizes the part of the nerve ending under the recording electrode or an as-yet-uncharacterized ionic current (4, 5, 29). (*C*) Effects of adenosine after cleavage of synaptobrevin with Botx/D in Rab3A$^{-/-}$ mutant (filled bar) are indistinguishable from those of maximal P/Q-type calcium channel block with Cd^{2+} (shaded bar). In contrast, the effects of Botx/D in the wild-type mouse (wt, open bar) are indistinguishable from the effects of adenosine in the absence of toxin treatment (see Fig. 3 in ref. 19). For further details, see the text.

significant inhibitory effect of supramaximal adenosine concentrations (10 mM) on the Ca^{2+} currents was observed in the Rab3A$^{-/-}$ mutant. These data and the statistically indistinguishable data obtained in the wild-type mouse (19) are depicted in Fig. 3 (Botx/C). These results indicate that syntaxin is an important target for inhibition by adenosine receptor activation in both the Rab3A$^{-/-}$ mutant and the wild-type mouse (19).

Effects of SNAP-25 Cleavage at Two Different Regions on the Actions of Adenosine. Because cleavage of the plasma membrane SNARE syntaxin eliminates the effects of adenosine, it would be of interest to determine whether cleavage of the other t-SNARE, SNAP-25 (Fig. 1), alters the effect of this GPCR agonist. SNAP-25 is loosely affiliated with the plasma membrane by palmitoylation. Botx/E irreversibly cleaves a 26-aa segment of SNAP-25 between amino acids R^{180} and I^{181} from the C terminus of the molecule (21–24) (Fig. 1). As shown in Figs. 2*C* and 3, after Botx/E treatment, adenosine failed to affect Ca^{2+} currents in preparations from either the wild-type or the Rab3A$^{-/-}$ mutant mouse.

It has been found that cleavage of SNAP-25 by Botx/E prevents the interaction of the G protein G$\beta\gamma$ subunits with SNAP-25 (10). In contrast, less extensive cleavage with Botx/A (Fig. 1), although reducing the affinity of G$\beta\gamma$ for SNAP-25, does not eliminate this interaction (10). It would be of interest to compare the effects of Botx/A, which irreversibly cleaves a 9-aa segment of SNAP-25 (between amino acids N^{197} and R^{198}) from the C terminus of the molecule (19, 21–24) (Fig. 1) with the more extensive 26-aa cleavage obtained with Botx/E. In contrast to the results with Botx/E, adenosine produced a statistically significant inhibition of Ca^{2+} currents after Botx/A treatment in each individual experiment ($P < 0.05$) in the Rab3A$^{-/-}$ mutant (mean percentage of inhibition after Botx/A treatment = 80.3% $\pm$ 2.1%, $n = 5$ experiments, Fig. 3). This effect of adenosine after Botx/A is indistinguishable from the maximal effects of adenosine in the absence of toxin treatment ($P = 0.54$, see Figs. 2*A* and 3) and after Botx/A treatment in the wild-type mouse (ref. 19; also see Fig. 3). It thus appears that the first nine amino acids at the C terminus are not required for the modulation of Ca^{2+} currents by adenosine at motor nerve endings, but that the adjacent 17 amino acids of SNAP-25 are essential for coupling A_1 adenosine receptor activation to the inhibition of Ca^{2+} currents.

Cleavage of Synaptobrevin Greatly Enhances the Efficacy of Adenosine in the Rab3A$^{-/-}$ Mutant but Not in the Wild-Type Mouse. As deletion of the vesicle protein Rab3A$^{-/-}$ increases the apparent affinity of adenosine as a modulator of Ca^{2+}currents (5), it appears of interest to determine whether the vesicle SNARE synaptobrevin (also known as vesicle associated membrane protein, or VAMP) can restrict the efficiency of GPRC modulation. To perform these experiments, synaptobrevin was cleaved by using Box/D (Fig. 1); Botx/D cleaves synaptobrevin between residues K^{59} and L^{60}, eliminates synaptobrevin immunoreactivity (24), and blocks the normal synchronous evoked release of Ach at vertebrate neuromuscular junctions (19, 30). As shown in Fig. 4*A*, after cleavage of synaptobrevin in the Rab3A$^{-/-}$ mutant, a dramatic and complete inhibition of the peak Ca^{2+} current was produced by adenosine (Fig. 4*A*, adenosine). Specifically, no statistically significant difference was observed between the peak of the residual outward current after the application of adenosine (56.7% $\pm$ 1%, $n = 5$ experiments, see Fig. 3's legend) or after the addition of the Ca^{2+} channel blocker Cd^{2+} (1 mM, 54.0% $\pm$ 3.45%, $n = 17$, $P = 0.68$) (Fig. 4*A*). This complete inhibitory effect of adenosine on the Ca^{2+} current was fully reversible (see Fig. 4*A*, 5- and 10-min wash periods). To illustrate the profound degree of inhibition produced by adenosine after Botx/D treatment in the mutant mouse, Fig. 4*B* shows a plot of the effects of adenosine on the normalized peak Ca^{2+} current (as a percentage of the control current, see Fig. 4's legend for further details). Note the essentially complete inhibition of the normalized P/Q calcium current by adenosine. Fig. 4*C* shows the mean results from all of the experiments made following cleavage of synaptobrevin after Botx/D treatment in Rab3A$^{-/-}$ mutant (black bar) as well as the Cd^{2+} -insensitive component of the perineural current peak (Fig. 4*C*, gray bar, Cd^{2+}). In contrast to the results in the Rab3A$^{-/-}$ mutant mouse, adenosine has its usual inhibitory effect after Botx/D cleavage in the wild-type mouse (83.0% $\pm$ 2.3% of control; Fig. 3*C*, open bar) (19). This increase in the efficacy of adenosine by synaptobrevin cleavage, which prevents the vesicle from participating in the priming process with the t-SNAREs, thus only occurs when vesicle docking is also reduced by the deletion of Rab3A.

Discussion

These results indicate that the maximal inhibitory effect of a GPCR agonist on membrane ionic currents can be increased by disruption of vesicle proteins. The effects of adenosine on Ca^{2+} currents after Botx/D treatment in the Rab3A$^{-/-}$ mutant are indistinguishable from those of concentrations of Cd^{2+}, which completely block Ach release (5). These data thus suggest that an endogenous mediator of presynaptic depression can have increased efficacy when vesicle proteins are deleted. They also

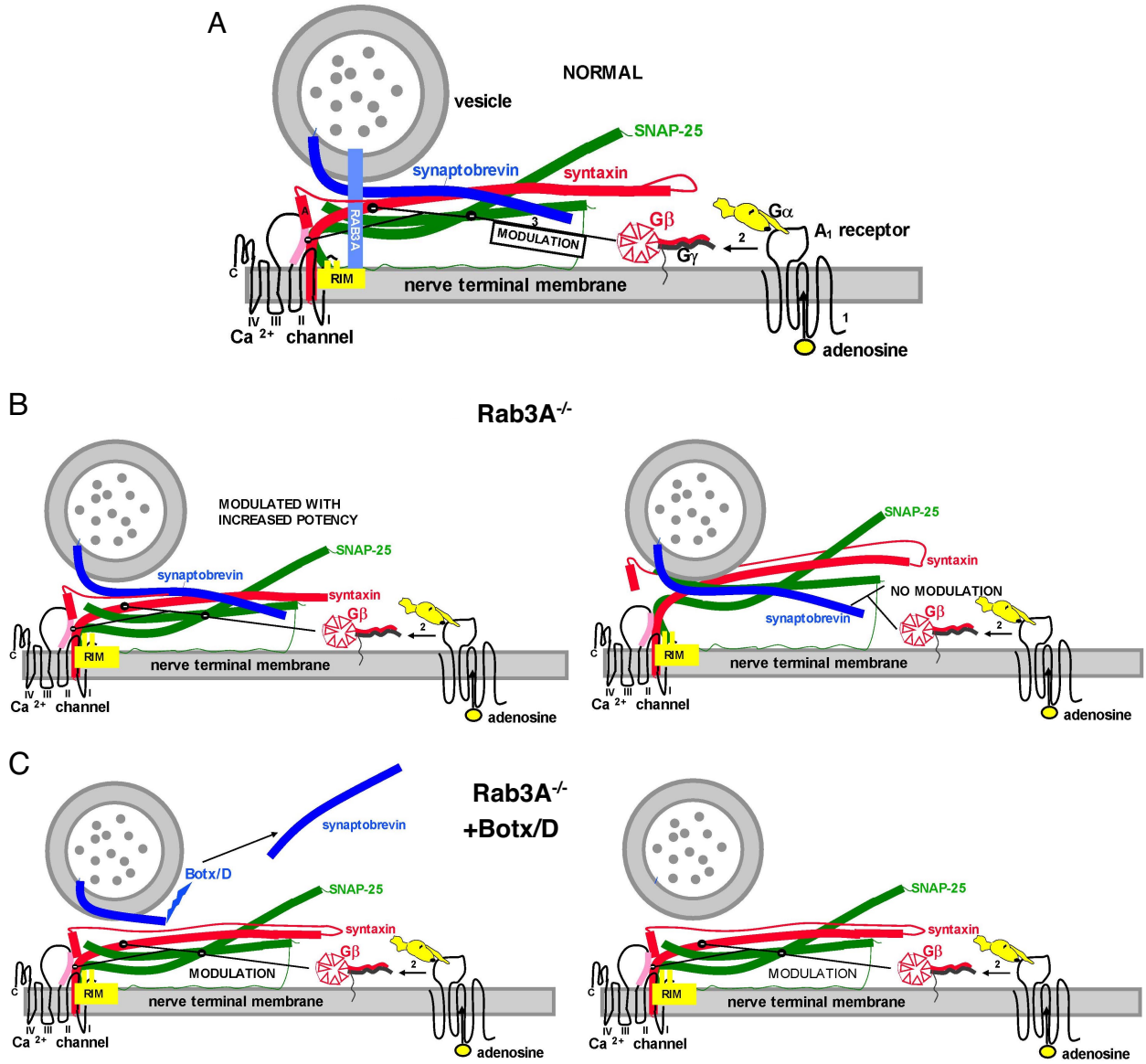

Fig. 5. A model for the enhanced effects of adenosine before and after disruption of vesicle proteins. (*A*) Same conditions as Fig. 1, but with the adenosine receptor and G protein included. The depiction of the G protein includes the β propeller region of Gβ that is believed to interact with effectors and the Gγ subunit with its prenylated attachment to the membrane (39). The Gα subunit was drawn in accordance with the crystal structure, with the receptor interaction domain and the GTP-binding region shown as a black circle and a black curving line, respectively. The helical domains are shown as ear-like appendages on the canine-like subunit. This figure also shows the N terminus of RIM interacting with Rab3A and two additional domains (C2 domains) that have been shown to interact with t-SNAREs and Ca^{2+} channels (40). For further details of the GPCR activation scheme for adenosine, see the text. (*B*) The situation in the Rab3A$^{-/-}$ mutant. Note the change in conformation in the SNARE complex in this mutant (*Left*) such that the complex has a higher affinity for Gβ. The SNARE- Ca^{2+} channel complex (*Right*) is not capable of being modulated by adenosine (no modulation). (*C*) The Rab3A$^{-/-}$ mutant after cleavage of synaptobrevin with Botx/D (*Left*). Note the recruitment of the additional site for modulation by adenosine by changes in conformation of the t-SNARE–Ca^{2+} channel complex when synaptobrevin is cleaved in the mutant mouse (*Right*, modulation). Recruitment of this site thus increases the level of inhibition of the macroscopic calcium currents. For further details of the synaptic proteins, see Fig. 1.

suggest that the maximal inhibitory effect of adenosine is not limited by the number of presynaptic adenosine receptors.

The results with Botx/A and Botx/E also demonstrate that nonselective disruption of a particular SNARE need not result in changes in GPCR modulation. Rather, it is the selective SNARE cleavage at discrete regions of the secretory apparatus that is necessary to affect the modulation of presynaptic Ca^{2+} currents. These data also provide an estimate of the minimal SNARE requirement for presynaptic modulation of calcium currents by adenosine, namely the cytoplasmic helical domains of syntaxin and a significant portion of SNAP-25 (excluding the last 9 amino acids at the C terminus).

A model for these results, based on these data and previously published results, is shown in Fig. 5. Fig. 5*A* depicts normal presynaptic modulation in the wild-type mouse, in which a vesicle is docked via GTP-bound Rab 3A to RIM at an active zone of secretion and primed via the SNARE complex (see also Fig. 1 for further details). Mechanistically, it is hypothesized that binding of adenosine to the A_1 adenosine receptor (marked as "1" in Fig. 5*A*) produces GTP/GDP exchange (not shown) and subsequently the dissociation of the G$\beta\gamma$ complex from the Gα subunit (marked as "2" in Fig. 5*A*). The G$\beta\gamma$ complex then interacts with the t-SNAREs syntaxin and SNAP-25 (marked as "3" in Fig. 5*A*), and

possibly with the Ca^{2+} channel (31, 32), and reduces Ca^{2+} channel activity and neurotransmitter release. Any interaction of Gβ with the Ca^{2+} channel requires obligatory binding to the t-SNAREs, however, because without these presynaptic membrane proteins, adenosine is incapable of modulating nerve terminal Ca^{2+} currents. In support of this model, previous results have demonstrated that it is the G$\beta\gamma$ subunits of GPCRs that interact with the secretory apparatus and calcium channels (9, 10, 31–39). Currently it is thought that G$\beta\gamma$ interacts with the Hcore (H3) helical domain of syntaxin (see Fig. 1 and refs. 10 and 32). However, a minor contribution from the other helical domains (HABC, Fig. 5*A*) is possible, either as a target for G$\beta\gamma$ (10, 19) or as a contributor to maintaining the optimal conformation of syntaxin for G$\beta\gamma$ binding (10, 32). The HA domain has been found to interact with Ca^{2+} channels (32), and this is depicted in Fig. 5*A* as well. This model is supported both by studies in which GTPγS is injected into the presynaptic element of the chick ciliary ganglion (34) and those from the lamprey in which G$\beta\gamma$ inhibited neurotransmitter release downstream of calcium entry (9, 10).

One possible explanation for the effects of Rab3A deletion and synaptobrevin cleavage is shown in Fig. 5 *B* and *C*, each depicting two release sites. In contrast to the normal situation in the wild-type mouse shown in Fig. 5*A*, deletion of Rab3A is envisaged as increasing the affinity of G$\beta\gamma$ for the SNARE–Ca^{2+} channel complex; this is reflected as an increased potency of adenosine (Fig. 5*B Left*). Speculatively, such an effect could be mediated by RIM (yellow), a protein that normally is intimately bound to Rab3A for docking but now is free to assist in the priming process via alterations in conformation of the t-SNARE–Ca^{2+} channel complex. Indeed, RIM has been found to interact with both t-SNARES and the pore-forming unit of calcium channels (40). Because of an unfavorable conformation of the t-SNARE–Ca^{2+} channel complex, the second release site and synaptic vesicle (Fig. 5*B Right*) is not capable of being modulated either in the wild-type (not shown) or in the Rab3A$^{-/-}$ mutant mouse (Fig. 5*B*, no modulation). After cleavage of synaptobrevin with Botx/D in the Rab3A mutant, a conformational change of the SNARE–Ca^{2+} channel complex occurs at the second, previously latent release site, such that modulation by adenosine at this site is now possible (Fig. 5*C Right*, modulation). This would be reflected as a greater level of inhibition of the macroscopically measured presynaptic Ca^{2+} currents. This hypothetical conformational change can occur only when Rab3A is deleted, again suggesting that a molecule such as RIM (or an alternative binding partner of Rab3A), when unencumbered from its interaction with Rab3A, can enhance the coupling between GPCR activation and the inhibition of presynaptic Ca^{2+} currents.

With respect to GPCR modulation in general, the maximal inhibitory effects of adenosine or other endogenous presynaptic GPCR agonists is usually limited to considerably less than complete inhibition at mammalian peripheral synapses (4, 5) and in the mammalian brain (ref. 11, but also see ref. 12). These present results provide a plausible explanation for such observations, namely that the vesicle components of a docked and primed vesicle are capable of limiting the maximal degree of presynaptic modulation via GPCRs. This type of regulation by the secretory apparatus would allow for restrictions to be placed on the maximum level of negative feedback inhibition of neurotransmitter release while at the same time ensuring the rapidity and fidelity of synaptic communication.

Materials and Methods

General Description of Preparations and Recording Methods. Isolated phrenic nerve hemidiaphragm preparations from Rab3A$^{-/-}$ mutant mice (B6,129-*Rab3A*tm1Sud; stock no. JR2443; The Jackson Laboratory, Bar Harbor, ME) were used in this study. Experiments were made in accordance with the guidelines of the Northwestern University Animal Care and Use Committee and the National Institutes of Health. Mice (20–30 g) were anesthetized with isoflurane. When unresponsive to tactile stimulation, the mice were then exsanguinated and the isolated preparations pinned in a recording chamber. Physiological saline solution at room temperature (21–23°C) was superfused by using a peristaltic pump (3.0 ml min^{-1}). Solutions were removed from the recording chamber by vacuum suction. Calcium currents were quantified by measuring voltage changes in the perineural space (5, 19, 25–29). The perineural recording electrodes were filled with normal physiological salt solution (3–10 MΩ) and positioned near small axon bundles at the heminode. The electrophysiological correlates of Ach secretion (EPPs; see Fig. 2*A*) were also recorded to monitor the elimination of Ach release (5, 19).

In response to phrenic nerve stimulation (generally 0.012–0.017 Hz), electrophysiological recordings were made by using an Axoclamp 2A, DigiData 1200, or TL-125 interface and pCLAMP software installed in a PC microcomputer (Axon Instruments). ASCII files from the pCLAMP recording were imported to Sigma Plot (Jandel Scientific) and then exported to Microsoft Power Point for lettering.

Botulinum Toxins. Isolated preparations were incubated with the specific serotype of botulinum toxin and rocked gently for 1 h in a shaker bath. The specific botulinum toxins and their concentrations were botulinum toxin type C (Botx/C, 56 μg ml^{-1}) type D (Botx/D, 7.8 μg ml^{-1}), type E (Botx/E, 15.6 μg ml^{-1}), and type A (Botx/A, 45–56 μg ml^{-1}). Preparations were then pinned in a tissue bath and stimulated at 1 Hz for $\approx$1 h (times ranged from 40 to 100 min). For specific details of the incubation protocols, the characteristic electrophysiological assessment of the selective cleavage by a particular fraction of botulinum toxin for its target SNARE, and for the toxin-free controls, see ref. 19 and supporting information (SI) *Text* and Fig. S1. For details of the morphological correlates of toxin treatment in mouse phrenic nerve endings, see ref. 24.

Physiological Saline Solutions. The standard control physiological saline solution used to treat the preparations before measuring calcium currents contained (in mM) NaCl 137, KCl 5, $CaCl_2$ 2, $MgCl_2$ 2, NaH_2PO_4 1, NaH_2HCO_3 24, dextrose 11, (pH 7.2–7.4 gassed with 95% O_2 and 5% CO_2). In the experiments in which Cd^{2+} was used, the physiological salt solutions were buffered with 30 mM Hepes (pH 7.2–7.4) and gassed with 100% O_2 to preclude the precipitation of divalent cations that may ensue with phosphate–bicarbonate solutions (19). These HEPES-buffered solutions contained (in mM) NaCl 137, KCl 5, dextrose 11, $CaCl_2$ 2 without NaH_2PO_4 or NaH_2HCO_3, and the K^+ channel blockers 3,4,-diaminopyridine (DAP, 300 μM) and tetraethylammonium (TEA, 10 mM) to expose the underlying Ca^{2+} currents. Botulinum toxin fractions were obtained from Wako Chemicals. All other chemicals were purchased from Sigma.

Perineural Ionic Currents. The perineural currents are, in actuality, voltage changes produced by ionic current flow across the resistance of the perineural sheath. The magnitudes of these currents are directly proportional to the difference in voltage between the nodes of Ranvier and the nerve endings. The inward Ca^{2+} current localized in the nerve terminals produces a proportional current in the perineural space, a current that flows back from the nerve ending to the recording site where it is measured as an upward (outward) deflection (5, 19, 25–29). Hence, although these are not strictly membrane ionic currents, the calcium component of the perineural waveform is directly linked to highly localized nerve terminal membrane Ca^{2+} conductance changes. Thus, for the sake of convenience, these waveforms will be termed "presynaptic Ca^{2+} currents" because they reflect an inverted replica of the localized ionic currents that develop in the nerve ending. More precisely, the term "Ca^{2+} current" will be used for the upward perineural voltage change that is antagonized by P- and Q-type Ca^{2+} channel blockers. Perineural waveforms are measured from the baseline to the peak of the current, and for the reasons stated above, the calibration bars are in millivolts (see refs. 5 and 19 for more details of the methods used to assess the stability of recordings).

Statistical Methods and Choice of Drug Concentrations. After testing the data for normality, statistical comparisons between control and treated cells were made by using the appropriate parametric or nonparametric statistical analysis (41). When more than two groups were compared for normally distributed data (e.g., Fig. 3), an analysis of variance was followed by multiple comparisons using the Bonferroni inequality (41). Data in Fig. 3 are presented as the mean $\pm$ SEM. For more complete details and justification, see the Methods in ref 19.

ACKNOWLEDGMENTS. I thank Dr. Timothy Searl for his suggestions and for a careful reading of the manuscripts, Dr. Paula Stern for her comments on the revised manuscript, Ms. Lauren Silinsky for her assistance with the design of the Gα canine subunit of Fig. 5, and Ms. Shirley Foster for her assistance with the dissections and the preparation of solutions. This is paper no. 4 in the Chair's Sanity Paper series. This work was supported by National Institutes of Health Grants NS 12782 and AA016513 and Northwestern Memorial Hospital.

1. Miller RJ (1998) Presynaptic receptors. *Annu Rev Pharmacol Toxicol* 38:201–227.
2. Scanziani M, Gahwiler BH, Thompson SM (1995). Presynaptic inhibition of excitatory synaptic transmission by muscarinic and metabotropic glutamate receptor activation in the hippocampus: Are Ca^{2+} channels involved? *Neuropharmacology* 34:1549–1557.
3. Silinsky EM (1984) On the mechanism by which adenosine receptor activation inhibits the release of acetylcholine from motor nerve endings. *J Physiol* (London) 346:243–256.
4. Hamilton BR, Smith DO (1991) Autoreceptor-mediated purinergic and cholinergic inhibition of motor nerve terminal calcium currents in the rat. *J Physiol* (London) 432:327–341.
5. Silinsky EM (2004) Adenosine decreases both presynaptic calcium currents and neurotransmitter release at the mouse neuromuscular junction. *J Physiol* (London) 558:389–401.
6. Silinsky EM, Solsona CS (1992) Calcium currents at motor nerve endings: Absence of effects of adenosine receptor agonists in the frog. *J Physiol* (London) 457:315–328.
7. Redman RS, Silinsky EM (1994) ATP released together with acetylcholine as the mediator of neuromuscular depression at frog motor nerve endings. *J Physiol* (London) 477:117–127.
8. Robitaille R, Thomas S, Charlton MP (1999) Effects of adenosine on Ca^{2+} entry in the nerve terminal of the frog neuromuscular junction. *Can J Physiol Pharmacol* 77:707–714.
9. Blackmer T, Larsen EC, Takahashi M, Martin TF, Alford S, Hamm HE (2001) G protein $\beta\gamma$ subunit-mediated presynaptic inhibition: Regulation of exocytotic fusion downstream of Ca^{2+} entry. *Science* 292:293–297.
10. Yoon E-J, Gerachskenko T, Spiegelberg BD, Alford S, Hamm HE (2007) G$\beta\gamma$ interferes with Ca^{2+}-dependent binding of synaptotagmin to the soluble *N*-ethylmaleimide-sensitive factor attachment protein receptor (SNARE) complex. *Mol Pharmacol* 72:1210–1219.
11. Straiker AJ, Borden CR, Sullivan JM (2002) G-protein alpha subunit isoforms couple differentially to receptors that mediate presynaptic inhibition at rat hippocampal synapses. *J Neurosci* 22:2460–2468.
12. Barnes-Davies M, Forsythe ID (1995) Pre- and postsynaptic glutamate receptors at a giant excitatory synapse in rat auditory brainstem slices. *J Physiol* (London) 488:387–406.
13. Ribeiro JA, Sebastiao AM (1987) On the role, inactivation and origin of endogenous adenosine at the frog neuromuscular junction. *J Physiol* (London) 384:571–585.
14. Meriney SD, Grinnell AD (1991) Endogenous adenosine modulates stimulation-induced depression at the frog neuromuscular junction. *J Physiol* (London) 443:441–445.
15. Redman RS, Silinsky EM (1993) A selective adenosine antagonist (8-cyclopentyl-1,3,-dipropylxathine) eliminates both neuromuscular depression and the action of exogenous adenosine by an effect on A_1 receptors. *Mol Pharmacol* 44:835–840.
16. Nagano O, *et al.* (1992) Presynaptic A_1-purinoceptor-mediated inhibitory effects of adenosine and its stable analogues on the mouse hemidiaphragm preparation. *Naunyn-Schmiedeberg's Arch Pharmacol* 346:197–202.
17. Hirsh JK, Searl TJ, Silinsky EM (2002) Regulation by Rab3A of an endogenous modulator of neurotransmitter release at mouse motor nerve endings. *J Physiol* (London) 545:337–343.
18. Silinsky EM, Redman RS (1996) Synchronous release of ATP and neurotransmitter within milliseconds of a motor nerve impulse in the frog. *J Physiol* (London) 492:815–822.
19. Silinsky EM (2005) Modulation of calcium currents is eliminated after cleavage of a strategic component of the mammalian secretory apparatus. *J Physiol* (London) 566 3:681–688.
20. Geppert M, Sudhof TC (1998) RAB 3 and synaptotagmin: The yin and yang of synaptic membrane fusion. *Annu Rev Neurosci* 21:75–95.
21. Jahn R, Hanson PI, Otto H, Ahnert-Hilger G (1995) Botulinum and tetanus neurotoxins: Emerging tools for the study of membrane fusion. *Cold Spring Harbor Symp Quant Biol* 60:329–335.
22. Simpson LL (1999) Botulinum toxin: Potent poison, potent medicine. *Hosp Pract* 34:87–91.
23. Raciborska DA, Trimble WS, Charlton MP (1998) Presynaptic protein interactions *in vivo*: Evidence from botulinum A, C, D, and E action at neuromuscular junctions. *Eur J Neurosci* 10:2617–2628.
24. Kalandakanond S, Coffield JA (2001) Cleavage of intracellular substrates of botulinum toxins A, C and D in a mammalian target tissue. *J Pharmacol Exp Ther* 296:749–755.
25. Brigant JL, Mallart A (1982) Presynaptic currents in mouse motor endings. *J Physiol* (London) 333:619–636.
26. Mallart A (1985) Electric current flow inside perineural sheaths of mouse motor nerves. *J Physiol* (London) 368:565–575.
27. Anderson AJ, Harvey AL, Rowan EF, Strong PN (1988) Effects of charybdotoxin, a blocker of calcium-activated potassium channels, on motor nerve terminals. *Br J Pharmacol* 95:1329–1335.
28. Protti DA, Uchitel OD (1993) Transmitter release and presynaptic Ca^{2+} currents blocked by the spider toxin ω-Aga-IVA. *NeuroReport* 5:333–336.
29. Xu X-F, Atchison WD (1996) Effects of omega-agatoxin-IVA and omega conotoxin-MVIIC on perineurial calcium and calcium-activated potassium currents of mouse motor nerve terminals. *J Pharmacol Exp Ther* 279:1229–1236.
30. Molgo J, Siegel LS, Tabti N, Thesleff S (1989) A study of synchronization of quantal transmitter release from mammalian motor nerve endings by the use of botulinal toxins type A and D. *J Physiol* (London) 411:195–205.
31. Catterall WA (2002) Structure and regulation of voltage-gated Ca $^{2+}$ channels. *Annu Rev Cell Dev Biol* 16:521–555.
32. Jarvis SE, Barr W, Feng Z-P, Hamid J, Zamponi GW (2002) Molecular determinants of syntaxin 1 modulation of N-type calcium channels. *J Biol Chem* 277:44399–44407.
33. Dolphin AC (2003) G-protein modulation of voltage gated calcium channels. *Pharmacol Rev* 55:607–627.
34. Stanley EF, Mirotznik RR (1997) Cleavage of syntaxin prevents G-protein regulation of presynaptic calcium channels. *Nature* 385:340–343.
35. Bezprozvanny I, Zhong P, Scheller RH, Tsien RW (2000) Molecular determinants of the functional interaction between syntaxin and N-type Ca^{2+}channel gating. *Proc Natl Acad Sci USA* 97:13943–13948.
36. Lu Q, *et al.* (2001) Syntaxin 1A supports voltage-dependent inhibition of alpha$_{1B}$ Ca^{2+} channels by G$\beta\gamma$ in chick sensory neurons. *J Neurosci* 21:2949–2957.
37. Harkins AB, Cahill AL, Powers AF, Tischler AS, Fox AP (2004) Deletion of the synaptic protein interaction site of the N-type ($Ca_v2.2$) calcium channel inhibits secretion in mouse pheochromocytoma cells. *Proc Natl Acad Sci USA*, 101:15219–15224.
38. Sutton RB, Fasshauer D, Jahn R, Brunger AT (1998) Crystal structure of the SNARE complex involved in synaptic exocytosis at 2.4 angstrom resolution. *Nature* 395:347–353.
39. Ford CE, *et al.* (1998) Molecular basis for interactions of G-protein beta gamma subunits with effectors. *Science* 280:1271–1274.
40. Coppola T, *et al.* (2001) Direct interaction of the Rab3 effector RIM with Ca^{2+} channels, SNAP-25 and synaptotagmin. *J Biol Chem* 276:32756–32762.
41. Glantz SA (1992) *Primer of Biostatistics* (McGraw–Hill, NY).